

## The evolution of the morphological scale of early-type galaxies since $z=2$

P. SARACCO<sup>(1)</sup>, M. LONGHETTI<sup>(1)</sup>, S. ANDREON<sup>(1)</sup>, A. MIGNANO<sup>(1)</sup> (\*)

<sup>(1)</sup> *INAF - Osservatorio Astronomico di Brera, Via Brera 28, 20121 Milano, Italy*

### Summary. —

We present the morphological analysis based on HST-NICMOS observations in the F160W filter of a sample of 30 early-type galaxies spectroscopically confirmed at  $1.2 < z < 2$ . We derive the effective radius  $R_e$  and the mean surface brightness  $\langle \mu \rangle_e$  of galaxies in the rest-frame R-band. We find that early-types at  $z \sim 1.5$  are characterized by a surface brightness much higher than their local counterparts with comparable  $R_e$ . In particular, we find that the mean surface brightness (SB) of these early-types should get fainter by  $\sim 2.5$  mag from  $z \sim 1.5$  to  $z \sim 0$  to match the SB of the local early-types with comparable  $R_e$ . This evolution exceeds by a factor two the luminosity evolution expected for early-types in this redshift range and more than a factor three the one derived from the observed luminosity function of galaxies. Consequently, an evolution of the effective radius  $R_e$  from the epoch of their formation towards  $z = 0$  has to be invoked and the hypothesis of fixed size rejected.

PACS 98.62 – evolution of galaxies, morphology, scaling relations.

PACS 98.52 – elliptical galaxies.

## 1. – Introduction

The formation and the evolution of early-type galaxies (ETGs, elliptical and bulge-dominated galaxies) occupy an important position among the challenges of the observational cosmology. At least  $\sim 70\%$  of the stellar mass in the local universe is locked into ETGs. For this reason, the understanding of their build-up and growth is fundamental to trace the galaxy mass assembly in the Universe. Evidence for a possible lack of large early-type galaxies at  $z \sim 1$  and beyond are coming out (e.g.[1, 2, 3]). At first glance, this could be interpreted as a prove of the merging process responsible of the growth of local high-mass ellipticals. On the other hand, the apparently smaller early-types seen at high-redshift are characterized by an effective surface brightness brighter than the local

---

(\*) Based on observations made with the NASA/ESA HST obtained at the Space Telescope Science Institute.

counterparts, i.e. they are more compact. However, most of these results are based on optical observations sampling the blue and UV rest-frame emission of the galaxies, particularly sensitive to morphological k-correction and star formation episodes, and/or on seeing limited ground-based observations. Here, we present the morphological analysis based on high-resolution (FWHM $\sim$ 0.1 arcsec) HST-NICMOS observations in the F160W filter ( $\lambda \sim 1.6 \mu\text{m}$ ) of a sample of 30 high-mass ETGs at  $1.2 < z < 2$ .

## 2. – The sample

The sample of ETGs we constructed is composed of 30 galaxies in the redshift range  $1.2 < z < 2$  with HST-NICMOS observations in the F160W ( $\lambda \sim 1.6 \mu\text{m}$ ) filter. In particular, images with the NIC2 (0.075 arcsec/pix) camera are available for 40% of the sample and with the NIC3 (0.2 arcsec/pix) camera for the remaining 60%.

The median redshift of the sample is  $z_{\text{med}} \simeq 1.4$ . Ten galaxies come from our own sample of ETGs spectroscopically confirmed at  $1.2 < z < 1.7$ . The study of their spectro-photometric and morphological properties based on multiwavelength data and HST-NICMOS observations are described in previous works [4, 2, 5]. The remaining 20 galaxies of the sample have been picked out from different surveys on the basis of their morphological classification and spectro-photometric properties. We restricted our selection to those galaxies having both deep HST-NICMOS observations and spectro-photometric confirmation of their redshift and spectral type. On the basis of these criteria we collected 14 ETGs with spectroscopic confirmation, 10 of which at  $1.4 < z < 1.9$  from the Galaxy Deep-Deep Survey (GDDS, [6]) and 4 at  $z \sim 1.27$  from the sample of Stanford et al.[7]. The remaining 6 ETGs have photometric redshift in the range  $1.2 < z < 2$  and they have been selected from the compilation of Moriondo et al.[8].

## 3. – The Kormendy relation and the evolution of the effective radius

The Kormendy relation (KR, Kormendy 1977) is a linear scaling relation between the logarithm of the effective radius  $R_e$  [Kpc], i.e. the radius containing half of the light, and the mean surface brightness  $\langle \mu \rangle_e$  [mag/arcsec<sup>2</sup>]:  $\langle \mu \rangle_e = \alpha + \beta \log(R_e)$

The ETGs follow this relation with a fixed slope  $\beta \sim 3$  up to  $z \sim 1$  [9] while the zero point  $\alpha$  varies with the redshift reflecting the luminosity evolution.

We derived the effective radius  $r_e$  (arcsec) and the mean surface brightness (SB)  $\langle \mu \rangle_e$  within  $r_e$  of our galaxies by fitting a Sersic profile to the observed light profiles. The analytic expression of the adopted profiles is  $I(r) = I_e \exp\{-b_n[(r/r_e)^{1/n} - 1]\}$  where  $n = 4$  and  $n = 1$  values define the de Vaucouleurs and to the exponential (disk) profiles respectively. We used galfit [10] to perform the fitting after the convolution of the images with the NIC2 and NIC3 PSFs. We used simulations [2] to assess the reliability of our estimate of  $r_e$ . We find that we underestimate  $r_e$  by about 0.05 arcsec in the NIC2 images and by about 0.03 arcsec in the NIC3 images while the typical rms is  $\sim 0.06$  arcsec ( $\sim 0.5$  Kpc at  $z \sim 1$ ). We derived  $R_e$  [kpc] from the values of  $r_e$  corrected for the underestimate and we converted the observed SB in the F160W filter into that in the rest-frame R-band using the proper k-correction for each galaxy (see [2] for details).

In Fig. 1 our galaxies (blue filled circles) at  $1.2 < z < 2$  are plotted on the  $[\mu_e, R_e]$  plane together with those from lower redshift samples. The thin (black) solid line is the observed KR in the R band at  $z \sim 0$  ( $\langle \mu \rangle_e = 18.2 + 2.92 \log(R_e)$ ) while the thick (red) line is the KR expected at  $z = 1.5$  ( $\langle \mu \rangle_e = 16.6 + 2.92 \log(R_e)$ ) in case of passive luminosity evolution (PLE). These two relations encompass the (yellow dashed) region

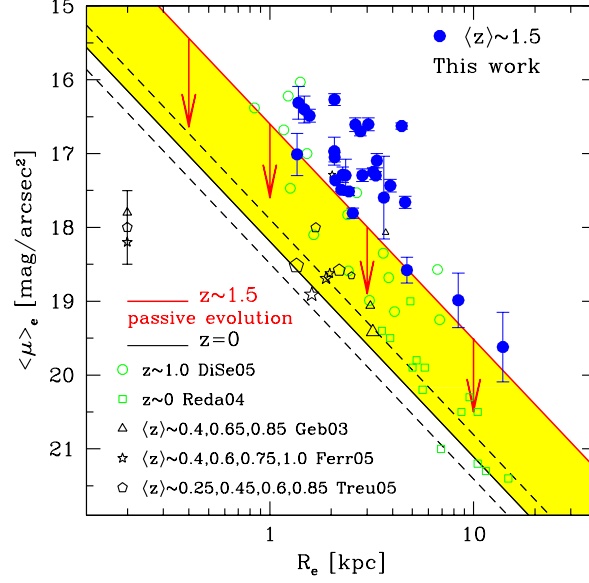


Fig. 1. – Mean surface brightness  $\langle \mu \rangle_e$  versus effective radius  $R_e$  [kpc]. The empty symbols are from the literature (see [2] for details). The thin solid line represents the KR at  $z \sim 0$  and the short-dashed lines represent the  $\pm 1\sigma$  dispersion of the relation. The thick (red) line is the KR expected at  $z \sim 1.5$  in case of PLE. All the data have been corrected for the cosmological dimming factor  $(1+z)^4$  thus, any deviation from the KR at  $z = 0$  reflects the evolution of the SB due to the luminosity and/or size evolution of galaxies.

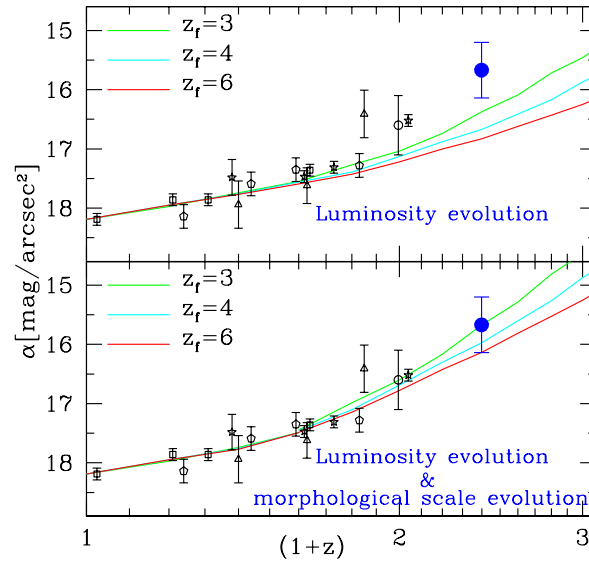


Fig. 2. – Zero points  $\alpha$  of the Kormendy relations derived by the various samples as a function of their redshift. Large filled circle represent the zero point we obtain from our sample. The lines show the expected evolution of  $\alpha$  due to the luminosity evolution alone (upper panel) and to the evolution of the morphological scale  $R_e$  in addition to the PLE (lower panel). Models refer to the same SFH  $\tau = 0.6$  Gyr starting at the redshifts of formation (from the top to the bottom)  $z_f = 3, 4, 6$ .

in the  $[\mu_e, R_e]$  plane where ETGs at  $z \sim 1.5$  are expected. However, all the ETGs of our sample drop out this region. Their surface brightness exceed by  $\Delta\langle\mu\rangle_e \simeq 1$  mag the one expected in the case of PLE for constant  $R_e$ .

In Fig. 2 the values of the zero point  $\alpha$  of the KR in the rest-frame R band derived from various samples at different redshift are shown and compared with the one expected in case of PLE (upper panel). It is evident the increasing discrepancy between the observed and the expected values of  $\alpha$  with increasing redshift, confirming that the luminosity evolution alone cannot reproduce the observed evolution of the KR from  $z \sim 1.5$  to  $z = 0$ . Thus, the other parameter involved in the KR relation, the effective radius  $R_e$ , must evolve and the hypothesis of fixed size must be rejected. A size evolution of at least a factor 2 from  $z \sim 1.5$  to  $z = 0$  is needed to account for the observed evolution of the KR. This is shown in the lower panel of Fig. 2 where the expected values of  $\alpha$  are shown in case of evolution of  $R_e$  in addition to the PLE.

#### 4. – Discussion and conclusions

ETGs at  $z \sim 1.5$  are characterized by a SB much higher then their local counterparts with comparable  $R_e$ . Luminosity evolution is able to account at most only for half of this excess. This means that the light of ETGs was actually much more concentrated (at least a factor two) in the past then in the present universe, i.e. that an evolution of  $R_e$  from the epoch of their formation towards  $z = 0$  has occurred. However, the appearance of a light profile can change due to both a variation of the spatial distribution of the stellar content or the presence of color gradients among the stellar populations. Thus a variation of  $R_e$  could coincide both with a variation of the stellar density (a contraction of  $R_e$  coincides with a contraction of the stellar system) or with different star formation histories affecting the outer and the inner regions of ETGs. Both these hypothesis are tightly linked to the formation of ETGs. Thus, the understanding of this evolution could open a new window in the comprehension of the formation of ETGs and on the assembly of the baryonic mass in the universe.

The complete analysis of the size evolution of this sample of ETGs and the possible dependence on their stellar mass will be presented in a forthcoming paper [11].

\* \* \*

This research has received financial support from the Istituto Nazionale di Astrofisica (Prin-INAF CRA2006 1.06.08.04)

#### REFERENCES

- [1] TRUJILLO I., FEULNER G., GORANOVA Y., ET AL., *MNRAS*, **373** (2006) 36;
- [2] LONGHETTI M., SARACCO P., SEVERGNINI P., ET AL., *MNRAS*, **374** (2007) 614;
- [3] TRUJILLO I., CONSELICE C. J., BUNDY K., ET AL., *MNRAS*, **in press** (2007) arXiv:0709.0621;
- [4] LONGHETTI M., SARACCO P., SEVERGNINI P., ET AL., *MNRAS*, **361** (2005) 897;
- [5] SARACCO P., LONGHETTI M., SEVERGNINI P., ET AL., *MNRAS*, **357** (2005) L40;
- [6] ABRAHAM R. G., GLAZEBROOK K., MCCARTHY P. J., ET AL., *AJ*, **127** (2004) 2455;
- [7] STANFORD S. A., ET AL., *AJ*, **114** (1997) 2232;
- [8] MORIONDO G., CIMATTI A., DADDI E., *A&A*, **364** (2000) 26;
- [9] DI SEREGO ALIGHIERI S., ET AL., *A&A*, **442** (2005) 125;
- [10] PENG C. Y., HO L. C., IMPEY C. D., RIX H.-W., *AJ*, **124** (2002) 266;
- [11] SARACCO P., LONGHETTI M., ET AL., in preparation